

SOURCE CODING OF AUDIO SIGNALS WITH A GENERATIVE MODEL

Roy Fejgin¹ Janusz Klejsa² Lars Villemoes² Cong Zhou¹

¹ Dolby Laboratories, San Francisco, CA, USA

² Dolby Sweden AB, Stockholm, Sweden

ABSTRACT

We consider source coding of audio signals with the help of a generative model. We use a construction where a waveform is first quantized, yielding a finite bitrate representation. The waveform is then reconstructed by random sampling from a model conditioned on the quantized waveform. The proposed coding scheme is theoretically analyzed. Using SampleRNN as the generative model, we demonstrate that the proposed coding structure provides performance competitive with state-of-the-art source coding tools for specific categories of audio signals.

Index Terms— audio coding, source coding, deep learning

1. INTRODUCTION

We propose a source coding scheme for audio employing a deep generative model that facilitates perceptually-optimized signal quantization with a seamless transition between waveform coding and parametric reconstruction of a coded signal. The scheme is capable of performing bandwidth extension, and of filling the reconstructed spectrum of a signal with plausible structures. In this paper, we provide two examples of scenarios where the proposed scheme outperforms state-of-the-art source coding techniques.

Deep generative models have been successfully used for speech coding [1–4], providing a significant improvement to the perceptual quality–bitrate tradeoff. These schemes comprised an encoder computing a parametric (finite bitrate) representation of speech, and a decoder based on a generative model. The speech signal was reconstructed by sampling from a learned probability distribution conditioned on the parametric representation.

Generative models were also used for synthesis of audio signals [5–7]. However, their application to audio coding remains an open problem. An application that is closest to the coding problem is a scheme of the Magenta Project [8], where piano waveforms were encoded into MIDI-like representation and then reconstructed from it. This conceptually resembles the mentioned speech coding schemes, where an encoder provides a salient parametric description of the signal to be generated. Perhaps the most obvious disadvantage of such an approach for audio is that the set of salient parameters would depend on signal category (e.g., MIDI-like parametrization would not be suitable to speech). In this work, we address this shortcoming by proposing a coding scheme that uses a generative model conditioned on quantized waveform. Specifically, we consider a source coding setup where a deterministic waveform coder is used to provide a finite-bitrate conditioning for a generative model at the decoder side.

Deep neural networks have already been applied to the audio coding problem in [9–11]. However, these schemes are based on discriminative networks. In contrast, generative modeling provides means for synthesis of plausible signal structures. This enhances

the perceptual performance at tasks such as bandwidth extension, or noise-fill by creating signal structures that would otherwise be lost due to signal quantization. Signal quantizers capable of providing source matching noise-filling were proposed in [12, 13]. However, these schemes were limited to scalar quantizers and used simple probability distributions describing the source.

This paper is organized as follows. In Section 2 we propose a source coding scheme for audio signals and provide its analysis. Then, in Section 3 we describe a practical coding scheme based on SampleRNN [6]. We evaluate its performance objectively and by means of listening tests in Section 4.

2. SOURCE CODING WITH A GENERATIVE MODEL

We study a coding scheme (shown in Fig. 1) consisting of a *waveform coder* and a generative model.

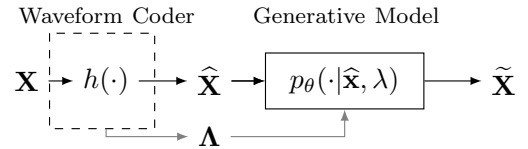


Fig. 1. Diagram of the proposed coding scheme.

We use upper case letters for random variables and lower case letters for their realizations. The waveform coder $h(\cdot)$ operates on signal samples blocked into vectors represented by \mathbf{X} , mapping \mathbf{x} to a waveform reconstruction $\hat{\mathbf{x}}$ and a set of parameters λ , both represented at a finite bitrate. The coder implements a bitrate–distortion tradeoff by using a sample distortion measure—here, perceptually-weighted squared error. The generative model provides a signal reconstruction $\tilde{\mathbf{x}}$ by random sampling from a conditional probability distribution $p_{\theta}(\cdot|\hat{\mathbf{x}}, \lambda)$ with parameters θ trained using a standard negative log-likelihood (NLL) loss.

In the following subsection, we analyze an idealized instance of the scheme. We first argue that the scheme tends to preserve the waveform match between \mathbf{X} and $\tilde{\mathbf{X}}$, which by itself is a useful property. It is then shown that, in the limit of increasing rate, the scheme incurs a performance loss in terms of sample distortion compared to a reconstruction with $\hat{\mathbf{X}}$. Interestingly, the distortion does not need to increase at low rates. Moreover, an increased sample distortion does not necessarily harm perceptual performance. A practical implementation is provided in Section 3, and finally the perceptual benefits are illustrated in Section 4.

2.1. Theoretical analysis

We will now discuss how the use of the NLL loss is related to the task of waveform coding. Each input signal in $\mathbf{x} \in \mathbb{R}^d$ is mapped

to $(\hat{\mathbf{x}}, \boldsymbol{\lambda}) = \mathbf{y} = h(\mathbf{x})$ by the (measurable) deterministic codec h . Due to the finite bitrate, the image $\mathcal{Y} = h(\mathbb{R}^d)$ consists of a finite set of points. If $\Omega_{\mathbf{y}} = \{\mathbf{x} : h(\mathbf{x}) = \mathbf{y}\}$ is the set of signals sharing the codec point \mathbf{y} , then $\cup_{\mathbf{y} \in \mathcal{Y}} \Omega_{\mathbf{y}}$ is a partition of \mathbb{R}^d . (In general $\Omega_{\mathbf{y}}$ can be a complicated high-dimensional object, but we will study a toy example in Section 2.2.) Assume $p(\mathbf{x})$ is the probability density of the signal source, and let $p_{\mathbf{y}}$ be the probability of $\Omega_{\mathbf{y}}$. Then

$$\begin{aligned} & \mathbb{E}_{\mathbf{X} \sim p(\cdot)} \{-\log p_{\theta}(\mathbf{X}) | h(\mathbf{X})\} \\ &= \sum_{\mathbf{y} \in \mathcal{Y}} p_{\mathbf{y}} \mathbb{E}_{\mathbf{X} \sim p(\cdot | \mathbf{y})} \{-\log p_{\theta}(\mathbf{X}) | \mathbf{y}\} \\ &\geq \sum_{\mathbf{y} \in \mathcal{Y}} p_{\mathbf{y}} \mathbb{E}_{\mathbf{X} \sim p(\cdot | \mathbf{y})} \{-\log p(\mathbf{X}) | \mathbf{y}\}, \end{aligned} \quad (1)$$

where the final inequality follows from the non-negativity of the Kullback-Leibler divergence, $\mathbb{KL}\{p(\cdot | \mathbf{y}) || p_{\theta}(\cdot | \mathbf{y})\} \geq 0$.

Viewing the left hand side of (1) as the idealized NLL loss, this shows that the training will encourage the parametric model $p_{\theta}(\mathbf{x} | \mathbf{y})$ to match the optimal conditional density $p(\mathbf{x} | \mathbf{y})$. An important property of this optimal case is that the resulting idealized scheme of Fig. 1 will preserve the distribution of the source. Another aspect is that *the noise shaping properties of the waveform coder will be inherited* since $p(\mathbf{x} | \mathbf{y}) = 0$ for $\mathbf{x} \notin \Omega_{\mathbf{y}}$, which often is a perceptually motivated vicinity of the original signal. In practical cases, the tradeoff between minimizing the probability mass outside of $\Omega_{\mathbf{y}}$ and achieving a good signal source match inside it is of course unknown.

The analysis of squared sample distortion in subspaces and with signal dependent perceptual weighting can be accommodated by using a positive semi-definite bilinear form depending on $h(\mathbf{x})$. If $\mu(\mathbf{z})$ is the expected value of \mathbf{X} in $\Omega_{h(\mathbf{z})}$, one can show, by using the partition $\cup_{\mathbf{y} \in \mathcal{Y}} \Omega_{\mathbf{y}}$ and the linearity of expectation, that

$$\begin{aligned} & \mathbb{E}\{\|\tilde{\mathbf{X}} - \mathbf{X}\|_{h(\mathbf{x})}^2\} \\ &= \mathbb{E}\{\|\mathbf{X} - \mu(\mathbf{X})\|_{h(\mathbf{x})}^2\} + \mathbb{E}\{\|\tilde{\mathbf{X}} - \mu(\mathbf{X})\|_{h(\mathbf{x})}^2\}, \end{aligned} \quad (2)$$

where expectations are with respect to the joint density $p(\tilde{\mathbf{x}}, \mathbf{x}) = p(\tilde{\mathbf{x}} | \mathbf{x}) p(\mathbf{x}) = p_{\theta}(\tilde{\mathbf{x}} | h(\mathbf{x})) p(\mathbf{x})$ of the coding scheme.

The first term on the right hand side of (2) is a (well-known) lower bound on the distortion, achieved by taking $\mu(\mathbf{X})$ as the reconstruction. For the NLL-optimal scheme $p_{\theta}(\cdot | h(\mathbf{x})) = p(\cdot | h(\mathbf{x}))$, the two terms of the right hand side of (2) are equal, resulting in a 3 dB loss of performance compared to $\mu(\mathbf{X})$,

$$\mathbb{E}\{\|\tilde{\mathbf{X}} - \mathbf{X}\|_{h(\mathbf{x})}^2\} = 2 \mathbb{E}\{\|\mathbf{X} - \mu(\mathbf{X})\|_{h(\mathbf{x})}^2\}. \quad (3)$$

Obviously, this loss also holds relative to a deterministic decoder with $\hat{\mathbf{x}} \approx \mu(\mathbf{x})$, which is more likely to happen in a high rate limit characterized by a flat signal distribution in $\Omega_{\mathbf{y}}$.

2.2. Toy example

To illustrate the concepts, we will study a synthetic example where the generative model outperforms the deterministic decoder. Hence, we are not in the high rate case outlined at the end of Section 2.1.

Let the signal source be random sines of unit amplitude, $x[k] = \cos[\pi(z_1 k + 2z_2)]$, $k = 1, \dots, d$, with z_1, z_2 i.i.d. uniformly distributed on $[0, 1]$, and let the waveform coder use scalar quantization with step size $\Delta > 0$ with midpoint reconstruction. This means that $\hat{x}[k] = \Delta \text{round}(x[k]/\Delta)$, and the sets $\Omega_{\mathbf{y}}$ are Voronoi cells of the quantizer which in this case are hypercubes of side length Δ in \mathbb{R}^d . For $d = 10$, it is feasible to implement $p(\mathbf{x} | \mathbf{y})$ by drawing random vector samples of \mathbf{x} until $\mathbf{x} \in \Omega_{\mathbf{y}}$. We estimated the left hand side of

(2), (without $h(\mathbf{X})$), by 10000 trials. For the generative model case we also created the mean over 10 realizations from $p(\mathbf{x} | \mathbf{y})$. The results normalized to per sample distortion are given in Table 1.

Table 1. Mean squared distortions for the toy example.

Δ	Midpoint	Sampling	Mean of 10 realizations
0.5	0.026	0.011	0.0056
1	0.11	0.068	0.038

As it can be seen, powerful signal source modeling leads to a significant advantage over the scalar midpoint quantizer. A comparison with (3) also reveals that the mean value of 10 samples approaches the optimum. However, one should keep in mind that among the three systems, only the middle one preserves the source distribution.

3. SOURCE CODING WITH SAMPLERNN

Next, we describe a practical implementation of the scheme discussed in Section 2. The scheme comprises a waveform codec operating in an MDCT domain and a generative model based on the SampleRNN [6], which is conditioned by waveform reconstructions obtained from the waveform codec.

3.1. Waveform coder

In this work we use a simple waveform coder operating in the MDCT domain, which is shown in Fig. 2. The input signal X is framed to facilitate application of an MDCT with a stride of 320 samples (at sampling frequency of $f_s = 16$ kHz). The coefficients of the transform are blocked into N non-uniform, non-overlapping frequency bands. For an n -th band, a variance of the coefficients is computed and quantized with a 3 dB step, yielding an index $i_{\text{env}}(n)$. The quantized values are blocked into a vector \mathcal{E} and coded into a bitstream using frequency differential coding with a Huffman codebook.

On the encoder side, the MDCT coefficients are first spectrally flattened by $F(\cdot)$ according to the envelope \mathcal{E} . The flattened MDCT lines are then quantized by a set of quantizers selected to fulfil a per-frame bitrate constraint. The set of quantizers $[m_0, \dots, m_M]$ is ordered providing incremental increases of SNR by 1.5 dB between each m_n and m_{n+1} . Each m_n is associated with a Huffman codebook.

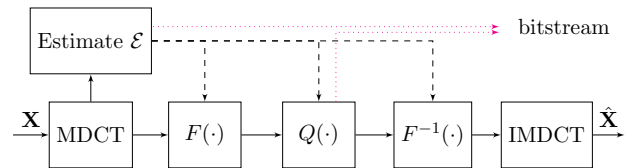


Fig. 2. Diagram of the waveform coder providing conditioning.

For every coded block, the rate allocation process is constrained by the total number of bits allocated to that block. It is controlled by $m_n = i_{\text{env}}(n) - i_{\text{offset}}$, where i_{offset} is an integer common to all the frequency bands and m_n is limited so that $0 \leq m_n \leq M$. The value of i_{offset} is determined by a binary search, which resembles the reverse water-filling procedure in a perceptually weighted domain. The perceptual effect of this rate allocation is that the SNR within a frame is allocated proportionally to the square root of the spectral envelope (allocating 1.5 dB SNR increase for every increase of the in-band envelope value by 3 dB).

On the decoder side, the MDCT lines are reconstructed in the flattened domain, and then the inverse spectral flattening $F^{-1}(\cdot)$ is applied. The inverse flattening is controlled by \mathcal{E} , which is decoded from the bitstream along with quantized transform coefficients and the rate allocation parameter i_{offset} .

3.2. Conditional SampleRNN

SampleRNN is a deep neural generative model proposed in [6] for generating raw audio signals by sampling them from a trained model $p_{\theta}(x)$. It consists of a series of multi-rate recurrent layers which are capable of modeling the dynamics of a sequence at different time scales and a multilayer perceptron (MLP) allowing usage of parameterized simple distributions.

SampleRNN models the probability of a sequence of audio samples blocked in \mathbf{x} by factorizing the joint distribution into the product of the scalar sample distributions conditioned on all previous samples. This facilitates an efficient implementation, where a single scalar sample is drawn at a time. Here we use a conditioned model $p_{\theta}(\mathbf{x}|\mathbf{y})$. The model operates recursively according to

$$p_{\theta}(\mathbf{x}|\mathbf{y}) = \prod_{i=1}^T p(x_i|x_1, \dots, x_{i-1}, \mathbf{y}). \quad (4)$$

We use a model similar to the one described in [2]. It is a four-tier SampleRNN with the conditioning provided to each tier through convolutional layers. We denote the frame size used by the k -th tier $\text{TS}^{(k)}$ ($1 \leq k \leq 4$) and denote the number of logistic mixture components L . The values of these hyperparameters are specified in section 4. The output layer utilizes the discretized mix of logistics technique [14] to generate 16-bit outputs. The differences to the model from [2] are as follows. The model here is conditioned on \mathbf{y} comprising frames of signal domain samples $\tilde{\mathbf{x}}$ reconstructed by the waveform codec and the associated values of the quantized signal envelope in \mathcal{E} (corresponding to λ in Fig. 1). The model operates with a look-ahead which improves the performance. This is done by processing the conditioning vector with 3×1 convolution layer, which results in a lookahead of two codec frames. Another difference to the model from [2] is an update to the MLP operation, where the MLP block, in addition to the conditioning described above, has access to the coded waveform processed through a convolutional layer utilizing a 319×1 kernel centered on the coded sample aligned with the prediction target. We use NLL as the training objective. We train the model using ADAM [15] with a learning rate of $2e-4$ and reduce the learning by a factor of 0.3 when the validation loss stops improving. In generation, we perform random sampling from the model.

4. EXPERIMENTS

In this section we provide results of subjective evaluation of the proposed source coding scheme in two coding tasks. The first task comprised coding of piano excerpts. The second task comprised coding of speech. In each of the tasks we compare the scheme against state-of-the-art codecs that are meant to represent source coding tools that would be typically used for the specific signal category considered in a coding task. We also provide examples and measurements corroborating the theory outlined in Section 2.

4.1. Subjective evaluation

In the first experiment we evaluate the proposed source scheme in a piano coding task. We trained the generative model using the

Maestro dataset [8], which was divided into non-overlapping training, validation and test sets. In order to provide the conditioning we used the waveform coder described in Section 3.1. SampleRNN (“sRNN”) was configured with $\text{TS}^{(1)} = 8$, $\text{TS}^{(2)} = 8$, $\text{TS}^{(3)} = 64$, $\text{TS}^{(4)} = 320$ and $L = 1$. We conducted a MUSHRA-like listening test [16] on the test set items, where we compared the proposed scheme against Opus [17] and AAC (which is a core of state-of-the-art audio codecs [18, 19]), and the baseline waveform (“Waveform”) coder operating at 16 kb/s. The conditions also included a hidden reference (16 kHz sampling) and a 3.5 kHz low pass anchor.

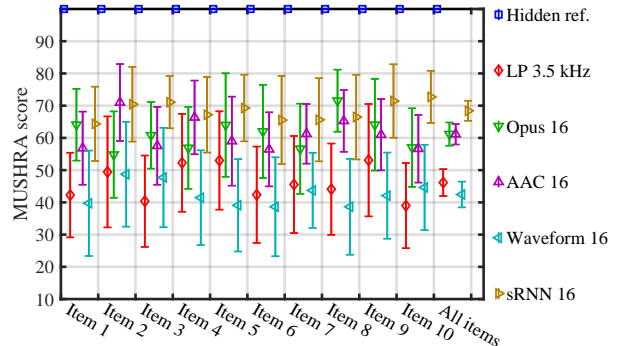


Fig. 3. Listening test results for Maestro piano (11 listeners, 95% confidence intervals, Student’s t-distribution).

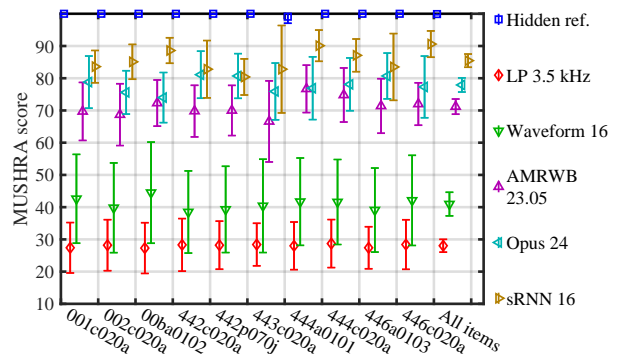


Fig. 4. Listening test results for WSJ0 speech (10 listeners, 95% confidence intervals, Student’s t-distribution).

The results of the first listening test are shown in Fig. 3. It can be seen that the proposed scheme significantly outperforms the baseline waveform coder, but also remains competitive to AAC. The advantage of AAC compared to Opus and the baseline waveform codec is due to its usage of window-switching, which facilitates usage of long MDCT transforms (64 ms stride) where it is perceptually advantageous.

In the second experiment, we evaluated the proposed scheme in a speech coding task. The results are shown in Fig. 4. In this case, we trained the generative model using the WSJ0 dataset [20] which was divided into training, validation and test sets with non-overlapping speakers. SampleRNN was configured with $\text{TS}^{(1)} = 2$, $\text{TS}^{(2)} = 2$, $\text{TS}^{(3)} = 16$, $\text{TS}^{(4)} = 160$ and $L = 10$. We performed a similar subjective test to the one in the previous experiment. This time the conditions included AMR-WB [21] at 23.05 kb/s (as it is

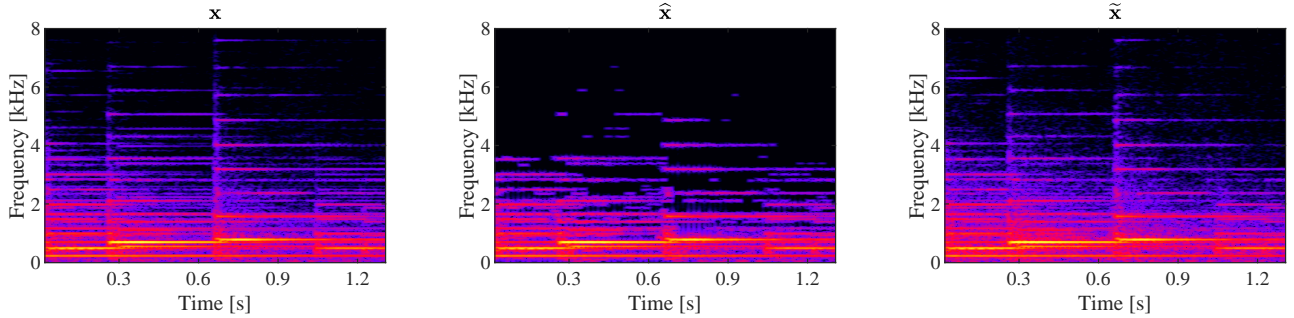


Fig. 5. Spectrograms: (left) reference \mathbf{x} ; (center) reconstruction from waveform codec $\hat{\mathbf{x}}$; (right) reconstruction of the proposed scheme $\tilde{\mathbf{x}}$.

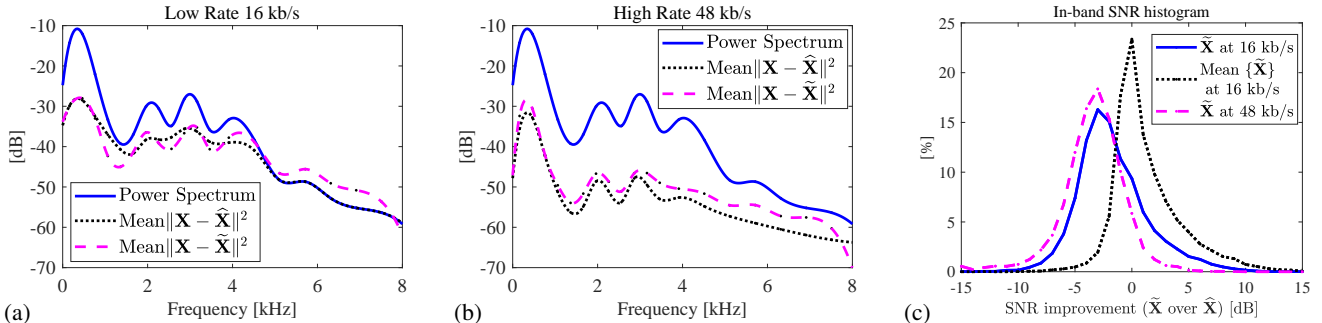


Fig. 6. Examples of a power spectrum of a signal segment and the corresponding power spectrum of sample distortion for (a) low rates and (b) high rates; (c) histograms of SNR improvement in bands of the waveform codec with respect to the waveform codec reconstruction.

a commonly included anchor in evaluation of speech codecs based on generative models), Opus at 24 kb/s; and also the baseline waveform codec and the proposed source coding scheme, both operating at 16 kb/s. It can be seen that the proposed scheme outperforms the waveform baseline by a large margin and that it remains competitive with the conditions representing state-of-the-art.

The significant perceptual advantage of the proposed scheme over the waveform baseline becomes apparent while inspecting spectrograms of the reconstructed signals. For example, in Fig. 5 we illustrate this for a signal from the piano coding experiment.

4.2. Objective measurements

An interesting property of the proposed scheme is that it allows some degree of control of spectral shaping of sample distortion even though the reconstructed signals are generated by random sampling. For example, the scheme described in Section 3 uses a waveform codec with a perceptual rule allocating the distortion proportionally to the square root of the frequency envelope of the signal. In Fig. 6a, we show an example of the power spectrum of a signal segment plotted along with the error spectrum of $\hat{\mathbf{X}}$ and the error spectrum of $\tilde{\mathbf{X}}$. It can be seen that the proposed source coding scheme closely follows the error shaping of the waveform codec. In the provided example, in the mid-frequency range the reconstruction with $\tilde{\mathbf{X}}$ had lower error. At high bitrates (see Fig. 6b) the noise shaping of the baseline waveform codec is still followed, but the average performance gap in terms of squared error grows to 3 dB when compared to the baseline waveform codec.

In order to provide an overview, we performed SNR measurements within the frequency bands of the baseline waveform codec and we compared the synthesis from SampleRNN to the baseline. The results were plotted as a histogram of SNR improvement over the waveform baseline in Fig. 6c. It can be seen that the histograms for the low rate case and for the high rate case are concentrated

around -3 dB. The histogram for the 16 kb/s version is more skewed towards the positive improvements likely due to the suboptimality of the baseline waveform codec at low rates. We note that while the scheme on average performs worse in terms of the SNR than the baseline, it provides a far superior perceptual performance.

The proposed interpretation of the scheme has predictive power. For example, one can expect that squared error performance could be improved by taking $\tilde{\boldsymbol{\mu}} = \mathbb{E}_{\tilde{\mathbf{x}} \sim p_{\theta}(\cdot|\mathbf{y})} \{\tilde{\mathbf{X}}\}$ as the reconstruction (if $p(\cdot)$ is approximated well by $p_{\theta}(\cdot)$). Since computing the expectation directly is difficult, instead we approximated $\tilde{\boldsymbol{\mu}}$ by averaging 10 realizations of $\tilde{\mathbf{X}}$. The result is shown in Fig. 6c, where it can be seen that not only was the 3 dB gap closed, but also the squared error performance improved over the baseline codec. This corroborates our theoretical interpretation of the scheme. We note that while such averaging can lead to an SNR improvement, this does not necessarily imply a perceptual improvement. In practice there is a non-trivial tradeoff between preservation of a waveform match and preservation of the distribution of the signal.

5. CONCLUSION

We proposed a source coding scheme based on a generative model that combines advantages of waveform coding and parametric coding in a seamless manner. When trained for a signal category, the scheme outperforms state-of-the-art source coding techniques. Moreover, the coding scheme can be used together with a perceptual model for allocating the coding distortion. The operation of the scheme and its performance can be described and predicted analytically.

6. ACKNOWLEDGMENT

The authors would like to thank Jordi Pons, Mark Vinton, Per Hedelin and Heiko Purnhagen for useful discussions and Richard Graff for help with listening tests.

7. REFERENCES

- [1] W. B. Kleijn, F. S. C. Lim, A. Luebs, J. Skoglund, F. Stimberg, Q. Wang, and T. C. Walters, "Wavenet based low rate speech coding," in *2018 IEEE International Conference on Acoustics, Speech and Signal Processing (ICASSP)*, April 2018, pp. 676–680.
- [2] Janusz Klejsa, Per Hedelin, Cong Zhou, Roy Fejgin, and Lars Villemoes, "High-quality speech coding with sample RNN," in *ICASSP 2019-2019 IEEE International Conference on Acoustics, Speech and Signal Processing (ICASSP)*. IEEE, 2019, pp. 7155–7159.
- [3] Jean-Marc Valin and Jan Skoglund, "A Real-Time Wideband Neural Vocoder at 1.6 kb/s Using LPCNet," *arXiv preprint arXiv:1903.12087*, 2019.
- [4] Jan Skoglund and Jean-Marc Valin, "Improving Opus low bit rate quality with neural speech synthesis," *arXiv preprint arXiv:1905.04628*, 2019.
- [5] Aaron van den Oord, Sander Dieleman, Heiga Zen, Karen Simonyan, Oriol Vinyals, Alex Graves, Nal Kalchbrenner, Andrew Senior, and Koray Kavukcuoglu, "Wavenet: A generative model for raw audio," *arXiv preprint arXiv:1609.03499*, 2016.
- [6] Soroush Mehri, Kundan Kumar, Ishaan Gulrajani, Rithesh Kumar, Shubham Jain, Jose Sotelo, Aaron Courville, and Yoshua Bengio, "SampleRNN: An unconditional end-to-end neural audio generation model," *arXiv preprint arXiv:1612.07837*, 2016.
- [7] Jesse Engel, Kumar Krishna Agrawal, Shuo Chen, Ishaan Gulrajani, Chris Donahue, and Adam Roberts, "Gansynth: Adversarial neural audio synthesis," *arXiv preprint arXiv:1902.08710*, 2019.
- [8] Curtis Hawthorne, Andriy Stasyuk, Adam Roberts, Ian Simon, Cheng-Zhi Anna Huang, Sander Dieleman, Erich Elsen, Jesse Engel, and Douglas Eck, "Enabling factorized piano music modeling and generation with the MAESTRO dataset," *arXiv preprint arXiv:1810.12247*, 2018.
- [9] Anton Porov, Eunmi Oh, Kihyun Choo, Hosang Sung, Jonghoon Jeong, Konstantin Osipov, and Holly Francois, "Music enhancement by a novel CNN architecture," in *Audio Engineering Society Convention 145*. Audio Engineering Society, 2018.
- [10] Seong-Hyeon Shin, Seung Kwon Beack, Taejin Lee, and Hochong Park, "Audio coding based on spectral recovery by convolutional neural network," in *ICASSP 2019-2019 IEEE International Conference on Acoustics, Speech and Signal Processing (ICASSP)*. IEEE, 2019, pp. 725–729.
- [11] Jun Deng, Björn Schuller, Florian Eyben, Dagmar Schuller, Zixing Zhang, Holly Francois, and Eunmi Oh, "Exploiting time-frequency patterns with LSTM-RNNs for low-bitrate audio restoration," *Neural Computing and Applications*, pp. 1–13, 2019.
- [12] Minyue Li and W Bastiaan Kleijn, "Quantization with constrained relative entropy and its application to audio coding," in *127th Audio Engineering Society Convention 2009; New York, NY; United States; 9 October 2009 through 12 October 2009*, 2009, pp. 401–408.
- [13] Minyue Li, Janusz Klejsa, and W Bastiaan Kleijn, "Distribution preserving quantization with dithering and transformation," *IEEE Signal Processing Letters*, vol. 17, no. 12, pp. 1014–1017, 2010.
- [14] Aaron van den Oord, Yazhe Li, Igor Babuschkin, Karen Simonyan, Oriol Vinyals, Koray Kavukcuoglu, George van den Driessche, Edward Lockhart, Luis C Cobo, Florian Stimberg, et al., "Parallel WaveNet: Fast high-fidelity speech synthesis," *arXiv preprint arXiv:1711.10433*, 2017.
- [15] Diederik P Kingma and Jimmy Ba, "ADAM: A method for stochastic optimization," *arXiv preprint arXiv:1412.6980*, 2014.
- [16] "Method for the subjective assessment of intermediate quality levels of coding systems," Recommendation ITU-R BS.1534-3, Oct. 2015.
- [17] Jean-Marc Valin, Koen Vos, and Timothy Terriberry, "Definition of the Opus audio codec," *RFC 6716, IETF*, 2012.
- [18] Jurgen Herre and Martin Dietz, "MPEG-4 high-efficiency AAC coding (standards in a nutshell)," *IEEE Signal Processing Magazine*, vol. 25, no. 3, pp. 137–142, 2008.
- [19] Schuyler Quackenbush, "MPEG unified speech and audio coding," *IEEE MultiMedia*, vol. 20, no. 2, pp. 72–78, 2013.
- [20] John S. Garofolo and et al., "CSR-I (WSJ0) complete LDC93S6A," Philadelphia: Linguistic Data Consortium, 1993.
- [21] B. Bessette, R. Salami, R. Lefebvre, M. Jelinek, J. Rotola-Pukkila, J. Vainio, H. Mikkola, and K. Jarvinen, "The adaptive multirate wideband speech codec (AMR-WB)," *IEEE Transactions on Speech and Audio Processing*, vol. 10, no. 8, pp. 620–636, Nov 2002.